

# Improved Generalizability of CNN Based Lane Detection in Challenging Weather Using Adaptive Preprocessing Parameter Tuning

I-Chen Sang, William R. Norris

Department of Industrial and Enterprise Systems Engineering  
University of Illinois Urbana-Champaign  
February 13, 2024

ichens2@illinois.edu , wrnorris@illinois.edu

## Abstract

Ensuring the robustness of lane detection systems is essential for the reliability of autonomous vehicles, particularly in the face of diverse weather conditions. While numerous algorithms have been proposed, addressing challenges posed by varying weather remains an ongoing issue. Geometric-based lane detection methods, rooted in the inherent properties of road geometry, provide enhanced generalizability. However, these methods often require manual parameter tuning to accommodate fluctuating illumination and weather conditions. Conversely, learning-based approaches, trained on pre-labeled datasets, excel in localizing intricate and curved lane configurations but grapple with the absence of diverse weather datasets.

This paper introduces a promising hybrid approach that merges the strengths of both methodologies. A novel adaptive preprocessing method is proposed in this work. Utilizing a fuzzy inference system (FIS), the algorithm dynamically adjusts parameters in geometric-based image processing functions and enhances adaptability to diverse weather conditions. Notably, this preprocessing algorithm is designed to seamlessly integrate with all learning-based lane detection models. When implemented in conjunction with CNN-based models, the hybrid approach demonstrates commendable generalizability across weather conditions and adaptability to complex lane configurations. Rigorous testing on datasets featuring challenging weather conditions showcases the proposed method's significant improvements over existing models, underscoring its efficacy in addressing the persistent challenges associated with lane detection in adverse weather scenarios.

## 1 Introduction

Advanced Driver Assistance Systems (ADAS) were introduced to vehicle systems in order to enhance efficiency and reduce the risks in driving. ADAS has been shown successful in reducing injury and deaths by sharing the workload of the drivers[1]. Common functions in ADAS are Lane Keeping Assistance systems (LKA), Adaptive Cruise Control (ACC), and Automatic Emergency Braking (AEB).

While ACC and AEB operate with distance estimation in the front, LKA tackles information that includes complicated road conditions and diversity of lane patterns. As a result, the lane detection function is a widely studied technology[2]. It is crucial for the research community to develop a lane detection algorithm that has high accuracy and adaptability for various weather conditions[3].

The lane detection task can be done by various sensors. Given the color and shape information in typical lines on the road, cameras are the most commonly used option. Several key features are commonly used in visual-based lane detection. For instance, the geometric attributes of lanes are often employed to eliminate erroneous candidates, utilizing the parallel nature of lane lines as a guiding principle[4]. On the other hand, color[5] and edge[3] features have been widely applied in lane detection algorithms because of the visual dissimilarity between the lines and asphalt.

Proximity sensors, such as LiDAR, are also promising in lane detection since the reflectivity of lane lines differs from that of asphalt. Studies have shown that the fusion between LiDAR and cameras can improve detection results compared to a single sensor.[6][7]

However, both proximity sensors and cameras are sensitive to weather changes. Specifically, when the road is covered with water on a rainy day, the reflectivity of the lines and asphalt becomes similar. The flowing raindrops

on the windshield, as well as the fast-moving wipers, pose extra difficulties for visual sensors[8][9]. As a result, a lane detection algorithm that can adapt to challenging weather conditions is needed to resolve this issue.

In this article, a preprocessing algorithm that is compatible with state-of-the-art lane detection frameworks is proposed. The algorithm consists of geometric-based modules with tunable parameters in order to adapt to different weather conditions. Two closed-loop feedback fuzzy logic modules are leveraged to tune the threshold values. With the noise-tolerant nature of fuzzy inference systems (FIS), the algorithm is able to overcome challenging weather conditions and provide more consistent inputs for learning-based lane detection convolutional neural networks (CNNs). With this innovative combination of geometric and learning-based methods, an improvement in the detection accuracy across multiple CNNs and datasets is presented, showing the effectiveness and robustness of the proposed algorithm.

This article is organized as follows: Section 2 delves into previous research and the challenges encountered in the field of lane detection. In Section 3, a comprehensive overview of the preprocessing algorithm, datasets employed, and the validation process is provided. Furthermore, Section 4 encompasses the presentation of experimental results and in-depth discussions. Finally, in Section 5, the article concludes by outlining the findings of this approach of this approach and discussing potential avenues for future research.

## 2 Related Work

Numerous works have been done in the lane detection field. These algorithms can be divided into geometric-based methods and learning-based methods.

### 2.1 Geometric-based methods

Geometric-based methods, also known as traditional approaches, utilize geometric features to identify the lines. For example, authors of [5] developed a method that was able to identify lane lines of different colors. The algorithm proposed in [2] adopted a clustering approach that correlated pixels with similar color and brightness. Other than color information, the edges of lines were leveraged in [3]. Thanks to the clear pattern in most road configurations, the geometric-based methods showed good generalizability and decent accuracy in the aforementioned works. Additionally, pre-trained models are not needed in these approaches.

Despite the strengths mentioned in the previous paragraph, challenges in several aspects still exist for traditional approaches. Geometric-based methods highly depend on brightness and color information and therefore require hand-tuning parameters to adapt to various conditions.

For example, the algorithm proposed in [10] showed a high accuracy of lane detection in rainy weather. However, after validation, it was found that the algorithm had difficulty working in lower illumination conditions unless the threshold was tuned manually. Furthermore, due to the complexity of curved lanes, many geometric-based studies are scoped on single, straight lanes [2][3][10].

### 2.2 Learning-based methods

On the contrary, learning-based methods utilize pre-collected and labeled data to attain precise detection. Throughout the training phase, these models deduce a set of parameters that yield optimal detection outcomes. Consequently, unlike traditional approaches, learning-based methods eliminate the need for manual parameter adjustments. Furthermore, learning-based methods take advantage of deep layers that process data at higher dimensions, providing benefits for image segmentation. As a result, learning-based models enable the handling of curved and multiple lines with greater efficacy.

Extensive learning-based algorithms have been published in the lane detection field. For instance, CLRNet[11] adopted a cross-layer approach to cover multi-scale features in the images, thereby achieving a high detection accuracy. RESA[12] dealt with the task with global features and performed pixel-wise identification. Different from standalone CNN models, authors of [13] introduced the Self-Attention Distillation (SAD) model to improve the performance of existing models, such as ResNet[14] and ENet[15]. All of the algorithms mentioned above showed successful detection results in multiple curved lanes.

Despite the adaptability to complicated line patterns, the difficulty faced in challenging weather conditions is seldom addressed in learning-based methods because of the considerable effort needed in data collection. An abundant lane detection dataset that includes various challenging weather conditions is needed to enhance the generalizability of the algorithms. However, many commonly used datasets, such as TuSimple[16], Caltech[17], and KITTI[18] were only collected in clear daylight. Efforts have been made to enhance the diversity of scenes in various datasets. For instance, the CULane dataset[19] introduced several weather conditions, encompassing nighttime and foggy scenarios. However, it notably lacked challenging images depicting rainy and snowy conditions. In contrast, the DSDLDE dataset[20], showcased a collection of 50 videos captured across a spectrum of weather conditions, spanning clear, rainy, and snowy weather. Regrettably, the official source did not include ground truth data.

In order to resolve the difficulty in data collection, works were proposed to raise the generalizability of learning-based methods. Authors of [21][22][23] trained the models

using the daytime data and applied the neural networks on the nighttime test sets. However, this approach has not been extended to rainy and snowy conditions yet. The other approach that deals with the limitation of datasets is data generation. Studies were proposed to generate nighttime[24] and foggy[25] images from clear daytime videos. This method has the potential to significantly increase the variety of datasets and therefore strengthen the robustness of learning-based methods. Nevertheless, the generative algorithms have not been applied in rainy and snowy weather conditions.

### 2.3 Hybrid methods

To combine the advantages of geometric-based and learning-based methods while addressing their limits, a hybrid approach is promising. Hybrid image processing algorithms have been applied to medical images. The work presented in [26] adopted both traditional quantitative image features and deep features that were extracted using pre-trained neural networks in a lung tumor detection task. The result showed that the accuracy was significantly improved compared to that using only traditional features and using only deep features. In addition, hybrid approaches were also leveraged in texture classification tasks. Authors of [27] applied the concept of traditional histogram calculation on feature maps in order to obtain the statistical information of the features. By introducing this “histogram layer”, a more accurate classification result was presented.

Similar attempts were also proposed in the lane detection field. The algorithm proposed in [28] incorporated traditional image preprocessing functions, such as range of interest (ROI) selection and inverse perspective transformation, with neural networks to conduct lane detection tasks. Moreover, the authors of [29] integrated the Adaptive Neuro-Fuzzy Inference System (ANFIS) with traditional geometric-based lane detection algorithms to achieve a better result. Both hybrid methods successfully combined the advantages of geometric-based and learning-based methods. However, the potential of the hybrid methods applied in lane detection algorithms’ adaptability to weather conditions has not been proposed yet.

As a result, a geometric-based adaptive preprocessing algorithm is presented in this article. When integrated with CNN-based lane detection models, the proposed function significantly improved multiple CNN models’ robustness over challenging weather conditions.

## 3 Methodology

This section presents the proposed preprocessing framework and all included functions in detail. In order to integrate with most lane detection models, the framework pro-

cessed color images and output images with the same size and number of channels.

The overall structure of the algorithm is shown in Figure 1. The input images were processed by the Noise reduction module, the Edge detection module, the ROI selection module, and the Line detection module sequentially. The threshold parameter in the Edge detection module was adjusted by a Fuzzy parameter tuner in each iteration. That is, the measurement acquired in frame  $N$  was processed by the parameter tuner which determined the parameter used in frame  $N + 1$ . The functionality and the details of each module are described in the paragraphs below.

- Noise reduction

To simplify the calculation, the images were transformed to grayscale when imported into the preprocessing module. A bilateral filter[30] was leveraged to suppress the noise in the images, enhancing the quality of the edge detectors. The bilateral filter calculated the weighted average of neighboring pixels with the weights determined by assigned spatial and color variance values. The mathematical expression of the bilateral filter was

$$K_{x_i}(x) = \frac{1}{W} \exp\left(\frac{\|x_i - x\|^2}{\sigma_s}\right) \exp\left(\frac{|I(x_i) - I(x)|^2}{\sigma_I}\right) \quad (1)$$

where  $x$  was the center pixel and  $x_i$  was the neighboring pixels in the kernel.  $\sigma_s$  and  $\sigma_I$  represented the pre-assigned variance value in space and intensity respectively, and  $W$  is the normalization parameter. A kernel size of  $7 \times 7$ , spatial variance of 50, and intensity variance of 25 were used in this work.

The contribution of the noise reduction module is shown in Figure 2. Figure 2(b) and (c) show the magnified image inside the red box before and after the filtering process, while (d) and (e) show the edge detection result. It is clear that the noise reduction module made a substantial improvement in the quality of the edge detection results. The erroneous detections resulting from image noise were effectively eliminated.

- Edge detection

After reducing the noise in images, a canny edge detection function[31] was utilized in this algorithm. The Canny edge detection function leveraged a  $3 \times 3$  filter to detect the gradient of the images in the x and y directions. The L2 summation of both gradient values then went through the non-maximum suppression before the thresholding process.

There were two threshold parameters required in the Canny edge detection function,  $Th_{high}$  and  $Th_{low}$ . The pixels with gradient values higher than  $Th_{high}$  were reserved while the ones lower than  $Th_{low}$  were deleted. On the other hand, the pixels with gradient values between

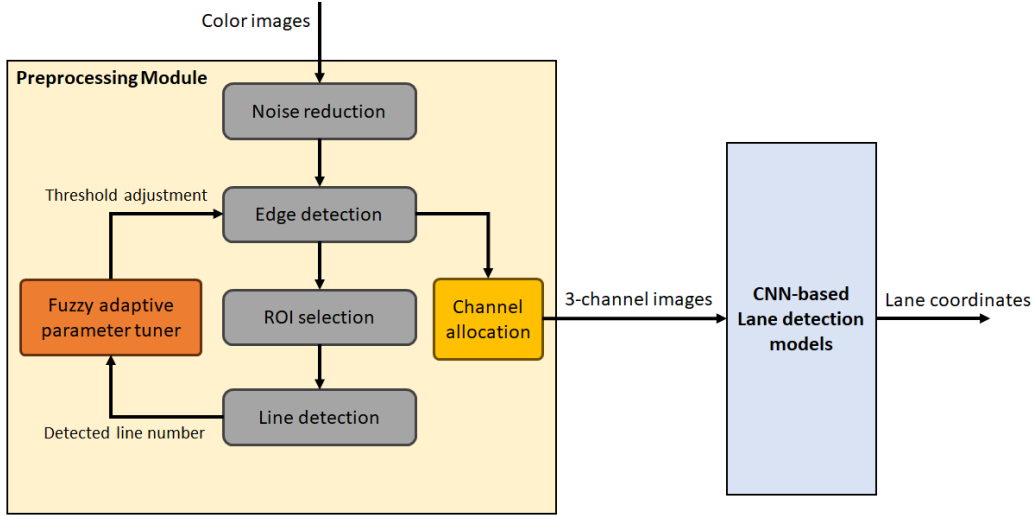


Figure 1: The flow chart for the overall structure is shown in this figure. The proposed preprocessing framework was connected with CNN-based lane detection algorithms

$Th_{high}$  and  $Th_{low}$  were only reserved when neighboring any candidates that were greater than  $Th_{high}$ . In this work,  $Th_{high}$  was adjusted by the fuzzy parameter tuner, and  $Th_{low}$  was  $1/3$  of  $Th_{high}$  as advised by [31].

- ROI selection

The number of candidate pixels hugely influenced the processing time of the preprocessing framework. In order to select better candidates among the edge pixels derived by the Canny edge detector, an ROI selection module was introduced.

Typical roads consist of parallel lines that converge to a vanishing point in images[4]. Therefore, with a triangular ROI, the possibility of capturing at least one lane in the image is high. When the slope is limited, the vanishing point resides around the center of the images. In this study, an ROI region that covers the vanishing point with a margin was adopted. Figure. 3 shows the edge detection result before (a) and after (b) the ROI selection process. The apex of the ROI was set at the center of the image with  $3/4$  of the image height.

- Line detection

A line detection function was incorporated into the process to tune the threshold of the Canny edge detection module. It was worth noting that the line detection result did not directly assist the lane detection process. Instead, it was leveraged as a measure to evaluate the performance of the current threshold value.

Considering the design of the triangular ROI and the typical structure of roads, it was expected that the ROI would

contain 1-2 lanes, which ranged from 1-3 line marks. As a result, when applying line detection modules, the detected line number should fall into a fixed range if the edge detection module is correctly tuned. To be more specific, when the edge detection module outputs more edge pixels than necessary, a higher detected line number is found; therefore, an increase in the threshold value is needed in this case.

The commonly used Hough Transform [32] was adopted to identify and quantify the line numbers in the images. The Hough Transform method generates straight lines in all directions, with each line centered on every edge pixel present in the images. A “vote” value is assigned to each line by tallying the number of edge pixels that align with the generated line. Lines with higher vote counts exhibit a stronger connection with edge pixels, thus making them preferred candidates for representing lane lines.

An angular resolution of 1 degree and a minimum intersection of 3 was adopted in this work. The detected line count was then used to tune the threshold value in the Canny edge detector, moderating the number of candidate pixels. The proposed closed-loop feedback process maintained a proper number of candidates, thereby eliminating the excessive processing time of Hough Transform.

- Fuzzy parameter tuner

An innovative parameter-tuning method is proposed in this work. Inspired by control algorithms where only “steering” decisions are output, the parameters were tuned relatively. To be more specific, the parameter tuner decided the direction (increase/decrease) and the level (more/less) of the applied change instead of outputting an absolute threshold value.



(a)



(b)



(c)



(d)



(e)

Figure 2: An example of the effect of the bilateral filter. Figure (b) and (c) show the magnified view of the red box in (a) before and after bilateral filtering. Figure (d) and (e) are the edge detection result of (b) and (c), respectively.

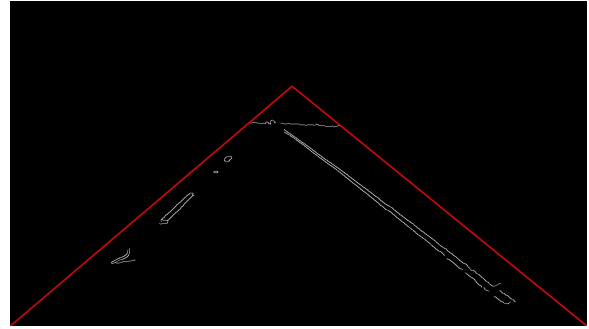
As mentioned previously, given the road structure and the inclusion of the ROI, the number of detected lines in the triangular ROI should fall into a fixed range. Therefore, the detected line number was leveraged as the “observable parameter” that could be used to tune the threshold value of Canny edge detector.

A Mamdani fuzzy inference system (FIS) was introduced in this process. FIS is based on rulebases that reflect human decisions. Therefore, fuzzy inference systems are also referred to as expert systems. Similar to human cognition processes, the input signals are fuzzified and labeled with linguistic variables before being processed by the rulebase. The linguistically labeled decisions made by the system are then defuzzified and projected to a numerical output value. The fuzziness of FIS increases the algorithm’s robustness when dealing with noises and the varying environment. In addition, the combination of linguistic variables and rulebases enables the users to design complicated projection functions intuitively.

A single input single output (SISO) FIS system was leveraged in the parameter tuning process. Five input mem-



(a)



(b)

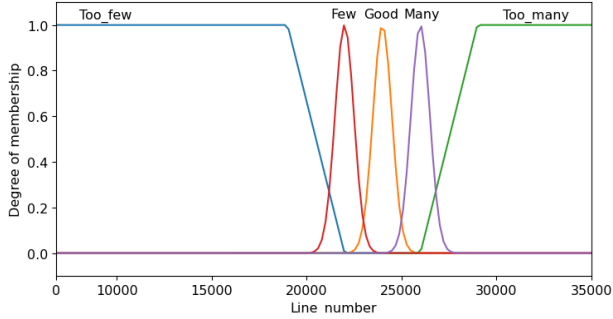
Figure 3: An example of the detection result of a frame before (a) and after (b) applying the triangular ROI.

bership functions (Fig. 4(a)) were defined according to the detected line count. Based on the membership functions, the probability of the input belonging to each linguistic category was calculated. The rulebase used in this work is listed in Table 1. When the line number detected was fewer than the expected value, the threshold of the Canny edge detector was reduced in order to introduce more information to the system and vice versa. The decisions made by the FIS were then defuzzified with the output membership functions (Fig. 4(b)).

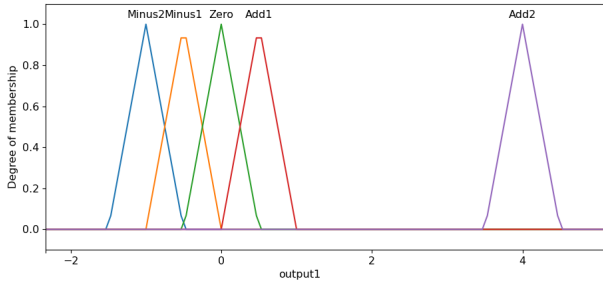
All membership functions were designed experimentally. The initial Canny threshold value was set to 1 in this work because it allows the most information from the images to be processed. However, to raise the threshold to the appropriate value effectively and thereby enhance the detection rate, an asymmetric design was adopted for the “Add2” function. This off-center function raised the threshold value quickly when the experiment was initiated, helping the system to stabilize within fewer frames.

- Channel allocation

At the end of the preprocessing algorithm, a channel allocation process was applied. Due to the adaptive parameter tuning capability of the algorithm, the edge detection result was able to outline the lane lines effectively. Therefore, the



(a)



(b)

Figure 4: The membership functions of the (a) input and (b) output of the threshold adjusting module.

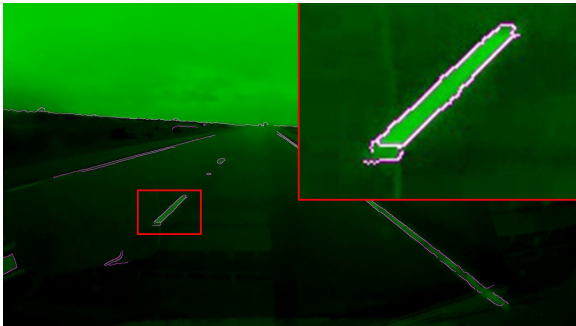


Figure 5: The result of the channel allocation process of the proposed method.

edge detection results were included in the final output to the CNN-based lane detection models.

Based on the experiments conducted, the green channel in the images carried more information on the white and yellow lines. Therefore, in the channel allocation process, the detected edge images were normalized to 8-bit and used to replace the red and blue channels of the original images. An example of the allocated result is shown in Figure 5. The figure shows that the green channel preserves most image features of the lines while the edge channels well-outlined the marks. This approach maintained the dimensions and the number of channels of the input image,

Table 1: The rule base of the fuzzy edge detection module.

Detected line number	Action to Canny threshold
Too few	Minus2
Few	Minus1
Good	Zero
Many	Add1
Too many	Add2

enabling seamless integration with most CNN-based lane detection models.

## 4 Experiment

To show the performance and the adaptability of the proposed preprocessing algorithm, the algorithm was incorporated with three different CNN-based lane detection models and tested on datasets with clear and rainy weather conditions. The details of the experiments are presented in detail in the following subsections.

### 4.1 Experiment setup

The experiment was designed to simulate the on-road driving conditions where all incoming images were processed sequentially. The validation experiments were performed using a PC with an Intel core i7, 3.2GHz CPU with 16GB RAM, and a GTX 1660 GPU with 16GB memory.

### 4.2 Datasets

- Tusimple[16]

The Tusimple dataset is a commonly used testbench in the lane detection field. It contains 6766 clips of 20 frames, with the last frame being labeled. Specifically, the training set encompasses 3626 clips, the validation set comprises 358 clips, and the test set encompasses 2782 clips. Notably, all images in the dataset are in RGB color format and exhibit a resolution of  $1280 \times 720$ .

Despite the uniform collection location being the highways of the United States, the Tusimple dataset exhibits a diverse array of line colors, configurations, and quantities. The dataset mostly captures bright and clear scenarios, with variations in the angles from which sunlight illuminates the scenes.

- DSDLDE[20]

The DSDLDE dataset specializes in the diverse weather conditions included. DSDLDE consists of 50 video clips,

where 27 were collected during daytime and 23 were captured during nighttime. The clips ranged from 900 to 2800 frames. In each category, three weather conditions (clear/rainy/snowy) were included. All images were at the resolution of  $1920 \times 1080$  at RGB color space.

Unlike the Tusimple dataset, the DSDLDE dataset was collected in both the United States and South Korea. A variety of scenes, including rural, city, caves, and highway, were covered. The dataset was constructed by multiple vehicles and camera setups. Therefore, different fields of view (FOV) were found in the dataset. For example, the area occupied by the hood or the interior of the vehicles ranged from 0 to roughly 40% of the images. Since this work is focused on algorithms’ adaptability across various weather conditions, efforts were made to simplify the comparison and focus on the weather variable. The images were cropped to an FOV that is similar to that of the Tusimple dataset and resized to  $1280 \times 720$ .

On the other hand, the biggest drawback of the dataset is the lack of labels and evaluation metrics. Therefore, to show the quantitative detection result of the DSDLDE dataset, a labeling GUI was made by the authors. The GUI assists the users in labeling any lane detection datasets and outputs the ground truths in the format of the Tusimple dataset, enabling quantitative comparison. The labeling GUI can be found at <https://github.com/ichensang/Lane-labeling>. The labeled results were uploaded to <https://github.com/ichensang/DSDLDE-labels>.

### 4.3 Training and testing process

The proposed preprocessing algorithm was integrated with three different CNN-based lane detection models and trained respectively. The models used in the experiment were CLNet-Resnet18[11], RESA[12], and Enet-SAD[13]. Since the DSDLDE dataset did not provide a training set, all models were only trained using the training set of the Tusimple dataset.

The initial setting of the parameters in the preprocessing algorithm was already covered in the Methodology section. On the other hand, most parameter settings for the lane detection models followed the original codes. Only the batch sizes were adjusted due to the limitations of the hardware. The batch sizes of CLNet-Resnet18, RESA, and Enet-SAD are 10, 4, and 5.

In order to simulate the scenario of an onboard driving task where the parameter tuner adjusts the threshold values with time, the testing process was revised accordingly. The test images were processed one at a time following sequential order. For the Tusimple dataset, the images in the test set were not continuous frames. Therefore, the images were processed sequentially according to the file names. The DS-



Figure 6: Example images of the DSDLDE dataset. (a), (b), and (c) are the mildly rainy cases while (d) and (e) are heavily rainy cases. (f) is the challenging cave scene included in the heavily rainy clips.

DLDE dataset, however, contained consecutive frames from multiple clips. So the test of the DSDLDE video clips was executed on a per-clip basis with the images processed sequentially with the timestamp.

Rainy samples from the DSDLDE dataset were used to test the algorithms’ adaptability toward different weather conditions. 5 video clips were selected from the “DayRain” category included in the DSDLDE dataset. All samples show visible raindrops on the windshield, significantly adding complexity to the lane detection task. According to the level that the lines were blurred by the raindrops, the 5 clips were further divided into “Standard rainfall” and “Heavy rainfall” categories. The example images of each category are shown in Figure. 6. The subfigures (a), (b), and (c) were captured from the “Standard rainfall” clips while (e) and (f) were from the “Heavy rainfall” category. Notably, Figure. 6 (g) shows a cave scenario captured from one of the Heavy rainfall samples. This scene added an additional challenge to the test dataset.

### 4.4 Evaluation metrics

To compare the results with previous research more effectively, the metrics of the Tusimple dataset were leveraged. All output from the CNN lane detection models was

Model	Dataset		
	Tusimple	DSDLDE Mild rain	DSDLDE Heavy rain
CLRNet	96.78	85.32	61.00
Proposed + CLRNet	96.64	95.00	69.66
RESA	96.78	84.48	58.93
Proposed + RESA	96.49	86.49	59.09
Enet-SAD	83.30	71.20	51.70
Proposed + Enet-SAD	91.50	88.55	59.73

Table 2: The accuracy of various models on the Tusimple dataset.

translated to the format of the ground truths provided by Tusimple and evaluated.

The metrics only considered the lane that the vehicle was in and the adjacent lanes on both sides. That is, the line quantity in the ground truths was capped at 4. Moreover, 56 y-coordinates were sampled on the images. The coordinates ranged from 160 to 710 with an increment of 10. Each detected line was expressed with an array of x-coordinates where it intersected with the above anchor coordinates. Each point in the detected line was compared with the x-coordinate of the ground truth. The accuracy of a line was derived by calculating the percentage of samples with a difference lower than a threshold value. The overall accuracy result was the average of all lines in the test dataset.

## 5 Results

### 5.1 The accuracy comparison with learning-based methods

The proposed preprocessing algorithm was integrated with CLRNet, RESA, and Enet-SAD and tested on both datasets. The result is shown in Table. 2.

The proposed preprocessing algorithm showed good compatibility with all three CNN-based lane detection models. By integrating the preprocessing algorithm, the detection performance of the models was significantly improved in rainy weather conditions despite a minor ( $< 1\%$ ) decrease in the clear daytime dataset.

It was observed that the edge detection function in the proposed algorithm was able to overcome the challenges posed by the raindrops. A significant improvement was thus observed in the mildly rainy scenario. In addition, the algorithm showed its capability to improve the detection result of the seriously blurred images collected under heavy rainy scenarios as well. Since the models were only trained in Tusimple dataset, this result also highlighted the increased generalizability contributed by the proposed algorithm.

Models	Accuracy(%)	Additional notes
CLRNet	84.86	
Proposed + CLRNet	95.81	
Lee[2]	96.9	Lowered standard while switching lanes
Ahmed[10]	92-97	Disregard switching lane images

Table 3: The accuracy of various dataset on the DSDLDE dataset

### 5.2 The accuracy comparison with geometric-based methods

The performance of the proposed algorithm was also compared with geometric-based methods mentioned in the previous section. Both research[2][10] considered only the closest two lines. Since the evaluation of [10] was conducted manually, the evaluation metrics of [2] were adopted in the comparison. According to Lee et al[2], the detected lines that overlap the lower 2/3 of the ground truth are defined as “detected”. When switching lanes, the allowed overlap region was increased by 50%. However, whether the vehicle is switching lanes cannot be clearly defined. The proposed algorithm was tested with the original standard on all images.

The comparison result is shown in Table. 3. All models were tested on the “DayRain” images from the DSDLDE dataset. The result shows that the accuracy of the proposed algorithm is similar to the previous works under a more difficult standard. In addition, the proposed algorithm was able to conduct multiple lane and curved lane detection tasks while geometric-based methods were limited to single straight lanes.

### 5.3 Processing time

The speed of the preprocessing algorithm was measured using the CPU mentioned above. Since the threshold value was tuned iteratively, and therefore influenced the processing time of each frame. The measurement was done by the average of 100 incoming frames. A frame rate of 23.8 was obtained in this experiment.

## 6 Conclusion

An innovative hybrid approach to lane detection was proposed in the work. The experimental result showed that the proposed framework was able to integrate with various CNN-based lane detection models. The fuzzy parameter

tuner provided a more informative input for the neural networks and therefore enhanced the generalizability and accuracy during challenging weather conditions.

More variations of hybrid image processing algorithms can be expected in future research. The fuzzy logic-based parameter tuner also has the potential to integrate with other geometric-based algorithms that require manual tuning. Furthermore, different approaches can be developed in the color space allocation function.

## References

- [1] B.-C. Chen, B.-C. Luan, and K. Lee, "Design of lane keeping system using adaptive model predictive control," in *2014 IEEE International Conference on Automation Science and Engineering (CASE)*, pp. 922–926, 2014.
- [2] C. Lee and J.-H. Moon, "Robust lane detection and tracking for real-time applications," *IEEE Transactions on Intelligent Transportation Systems*, vol. 19, no. 12, pp. 4043–4048, 2018.
- [3] S. Sultana, B. Ahmed, M. Paul, M. R. Islam, and S. Ahmad, "Vision-based robust lane detection and tracking in challenging conditions," *IEEE Access*, vol. 11, pp. 67938–67955, 2023.
- [4] S. Luo, X. Zhang, J. Hu, and J. Xu, "Multiple lane detection via combining complementary structural constraints," *IEEE Transactions on Intelligent Transportation Systems*, vol. 22, no. 12, pp. 7597–7606, 2021.
- [5] Q. Lin, Y. Han, and H. Hahn, "Real-time lane departure detection based on extended edge-linking algorithm," in *2010 Second International Conference on Computer Research and Development*, pp. 725–730, IEEE, 2010.
- [6] Q. Li, L. Chen, M. Li, S.-L. Shaw, and A. Nüchter, "A sensor-fusion drivable-region and lane-detection system for autonomous vehicle navigation in challenging road scenarios," *IEEE Transactions on Vehicular Technology*, vol. 63, no. 2, pp. 540–555, 2013.
- [7] Z. Chen, J. Zhang, and D. Tao, "Progressive lidar adaptation for road detection," *IEEE/CAA Journal of Automatica Sinica*, vol. 6, no. 3, pp. 693–702, 2019.
- [8] M. Aldibaja, N. Suganuma, and K. Yoneda, "Improving localization accuracy for autonomous driving in snow-rain environments," in *2016 IEEE/SICE International Symposium on System Integration (SII)*, pp. 212–217, IEEE, 2016.
- [9] C. Rose, J. Britt, J. Allen, and D. Bevlly, "An integrated vehicle navigation system utilizing lane-detection and lateral position estimation systems in difficult environments for gps," *IEEE Transactions on Intelligent Transportation Systems*, vol. 15, no. 6, pp. 2615–2629, 2014.
- [10] S. Sultana and B. Ahmed, "Lane detection and tracking under rainy weather challenges," in *2021 IEEE Region 10 Symposium (TENSYP)*, pp. 1–6, IEEE, 2021.
- [11] T. Zheng, Y. Huang, Y. Liu, W. Tang, Z. Yang, D. Cai, and X. He, "Clnet: Cross layer refinement network for lane detection," in *Proceedings of the IEEE/CVF conference on computer vision and pattern recognition*, pp. 898–907, 2022.
- [12] T. Zheng, H. Fang, Y. Zhang, W. Tang, Z. Yang, H. Liu, and D. Cai, "Resa: Recurrent feature-shift aggregator for lane detection," in *Proceedings of the AAAI Conference on Artificial Intelligence*, vol. 35, pp. 3547–3554, 2021.
- [13] Y. Hou, Z. Ma, C. Liu, and C. C. Loy, "Learning lightweight lane detection cnns by self attention distillation," in *Proceedings of the IEEE/CVF International Conference on Computer Vision (ICCV)*, October 2019.
- [14] K. He, X. Zhang, S. Ren, and J. Sun, "Deep residual learning for image recognition," in *Proceedings of the IEEE conference on computer vision and pattern recognition*, pp. 770–778, 2016.
- [15] A. Paszke, A. Chaurasia, S. Kim, and E. Culurciello, "Enet: A deep neural network architecture for real-time semantic segmentation," *arXiv preprint arXiv:1606.02147*, 2016.
- [16] "Tusimple benchmark." <https://github.com/TuSimple/tusimple-benchmark/issues/3>. Accessed: 2023-06-06.
- [17] M. Aly, "Real time detection of lane markers in urban streets," in *2008 IEEE Intelligent Vehicles Symposium*, pp. 7–12, 2008.
- [18] A. Geiger, P. Lenz, and R. Urtasun, "Are we ready for autonomous driving? the kitti vision benchmark suite," in *2012 IEEE Conference on Computer Vision and Pattern Recognition*, pp. 3354–3361, 2012.
- [19] X. Pan, J. Shi, P. Luo, X. Wang, and X. Tang, "Spatial as deep: Spatial cnn for traffic scene understanding," in *Proceedings of the AAAI Conference on Artificial Intelligence*, vol. 32, 2018.

- [20] “DSDLDE v.0.9: Video clips for lane marking detection.”
- [21] M. M. Yusuf, T. Karim, and A. S. Saif, “A robust method for lane detection under adverse weather and illumination conditions using convolutional neural network,” in *Proceedings of the International Conference on Computing Advancements*, pp. 1–8, 2020.
- [22] Y. Dong, S. Patil, B. van Arem, and H. Farah, “A hybrid spatial–temporal deep learning architecture for lane detection,” *Computer-Aided Civil and Infrastructure Engineering*, vol. 38, no. 1, pp. 67–86, 2023.
- [23] Y. Lee, J. Lee, Y. Hong, Y. Ko, and M. Jeon, “Unconstrained road marking recognition with generative adversarial networks,” in *2019 IEEE Intelligent Vehicles Symposium (IV)*, pp. 1414–1419, 2019.
- [24] T. Liu, Z. Chen, Y. Yang, Z. Wu, and H. Li, “Lane detection in low-light conditions using an efficient data enhancement: Light conditions style transfer,” in *2020 IEEE Intelligent Vehicles Symposium (IV)*, pp. 1394–1399, 2020.
- [25] X. Nie, Z. Xu, W. Zhang, X. Dong, N. Liu, and Y. Chen, “Foggy lane dataset synthesized from monocular images for lane detection algorithms,” *Sensors*, vol. 22, no. 14, p. 5210, 2022.
- [26] R. Paul, S. H. Hawkins, L. O. Hall, D. B. Goldgof, and R. J. Gillies, “Combining deep neural network and traditional image features to improve survival prediction accuracy for lung cancer patients from diagnostic ct,” in *2016 IEEE International Conference on Systems, Man, and Cybernetics (SMC)*, pp. 002570–002575, 2016.
- [27] J. Peeples, W. Xu, and A. Zare, “Histogram layers for texture analysis,” *IEEE Transactions on Artificial Intelligence*, vol. 3, no. 4, pp. 541–552, 2021.
- [28] J. Li, D. Zhang, Y. Ma, and Q. Liu, “Lane image detection based on convolution neural network multi-task learning,” *Electronics*, vol. 10, no. 19, p. 2356, 2021.
- [29] A. Küçükmanisa, O. Akbulut, and O. Urhan, “Robust and real-time lane detection filter based on adaptive neuro-fuzzy inference system,” *IET Image Processing*, vol. 13, no. 7, pp. 1181–1190, 2019.
- [30] C. Tomasi and R. Manduchi, “Bilateral filtering for gray and color images,” in *Sixth international conference on computer vision (IEEE Cat. No. 98CH36271)*, pp. 839–846, IEEE, 1998.
- [31] J. Canny, “A computational approach to edge detection,” *IEEE Transactions on pattern analysis and machine intelligence*, no. 6, pp. 679–698, 1986.
- [32] P. V. Hough, “Method and means for recognizing complex patterns,” Dec. 18 1962. US Patent 3,069,654.